Full-speed ahead all-electric proton EDM ring

Richard Talman
Laboratory for Elementary-Particle Physics
Cornell University

15 January, 2018, Juelich

2 Outline

3 EDM task force: Talman lecture schedule

- Day 1: Full-speed ahead all-electric proton EDM ring
- Day 2: Cautious prototype EDM plan;
- Day 3: Weak-weaker/weak/strong focusing; review (beautiful) Valeri Lebedev 2015 paper
- Day 4: A more ambitious proton EDM-prototype ring
- Day 5: Review
- Day 6: Spin evolution and coherence
- Day 7: Polarimetry
- Day 8: TBD
- Day 9: TBD
- Day 10: TBD

4 Extending historical force field symmetry studies

The measurement of electric dipole moments (EDMs) of elementrary particles would provide a modest extension to our understanding of force field symmetries. The most important of these historical milestones can be encapsulated in the following list:

- Newton: Gravitational field, (inverse square law) central force
- Coulomb: By analogy, electric force is the same (i.e. central, $1/r^2$)
- Ampere: How can a compass needle near a current figure out which way to turn? A *right hand rule* is somehow built into E&M and into the compass needle. Mathematically this requires the magnetic field to be a *pseudo-vector*.
- The upshot: by introducing *pseudo-vector* magnetic field, E&M respects reflection symmetry. This was the first step toward the *grand unification* of all forces, which culminated eventually in Maxwell's completion of electromagnetic theory.

5 History (continued)

- Lee, Yang, etc: A particle with spin (*pseudo-vector*), say "up", can decay more up than down (*vector*);
  - i.e. the decay vector is parallel (not anti-parallel) to the spin pseudo-vector,
  - viewed in a mirror, this statement is reversed.
  - i.e. weak decay force violates reflection symmetry (P).
- Fitch, Cronin, etc: standard model violates both parity (P) and time reversal (T), (so protons, etc. must, at some level, have non-vanishing EDM).
- Current task: How to exploit the implied symmetry violation to measure the EDM of proton, electron, etc?

6 EDM Sensitive Configuration—modern day Ampère experiment

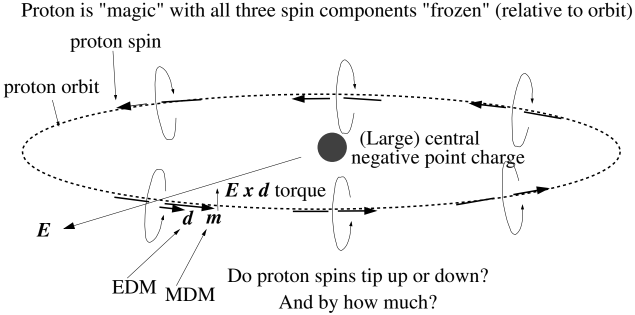

Two issues:

- Can the tipping angle be measurably large for plausibly large EDM, such as 10^{-30} e-cm? With modern technology, yes
- Can the symmetry be adequately preserved when the idealized configuration above is approximated in the laboratory? *This is the main issue*

The very smallness of EDMs that makes measuring them so important, makes the measurement difficult, or even impossible?

7 Two experiments that “could not be done”

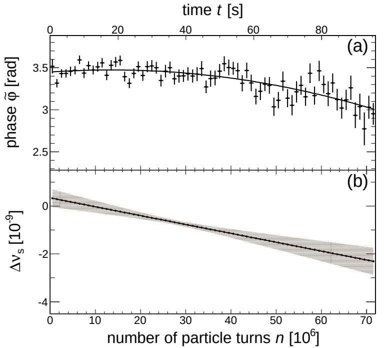

FIG. 3. (a): Phase $\tilde{\varphi}$ as a function of turn number n for all 72 turn intervals of a single measurement cycle for $\nu_s^{\text{fix}} = -0.160975407$, together with a parabolic fit. (b): Deviation $\Delta\nu_s$ of the spin tune from ν_s^{fix} as a function of turn number in the cycle. At $t \approx 38$ s, the interpolated spin tune amounts to $\nu_s = (-16097540771.7 \pm 9.7) \times 10^{-11}$. The error band shows the statistical error obtained from the parabolic fit, shown in panel (a).

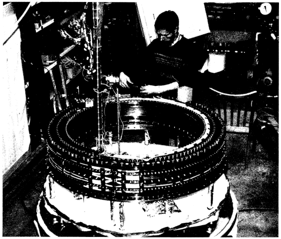

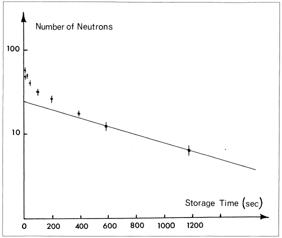

Figure 1: COSY, Juelich, Eversmann et al.: (Pseudo-)frozen spin deuterons, and Bonn, Paul et al.: neutron storage ring

Remarkable coincidence

We can also include two experiments that “were not even thinkable” at the time they were performed.

- Franfurt: Stern-Gerlach experiment—1923, beginning of quantum mechanics (shortly after Hans Bethe had transferred from there to Munich to complete his PhD, and before he returned in 1928—Rose (Ewald) Bethe knew Gerlach)
- Aachen: first RF accelerator—1927, Wideroe PhD thesis, beginning of high energy physics

Remarkable coincidence!

- All four impossible experiments were performed in the same general area—central Rhine
- Should be designated “Cultural heritage treasure”
- Science is “culture”
- Politicians can understand this
- Even scientists should be able to understand it

The challenge is to succeed in performing another “impossible” experiment

9 Why all-electric ring?

- "Frozen spin" operation in all-electric storage ring is only possible with electrons or protons—by chance their anomalous magnetic moment values are appropriate. The "magic" kinetic energies are 14.5 MeV for e, 233 MeV for p.
- Beam direction reversal is possible in all-electric storage ring, with all parameters except injection direction held fixed. This is crucial for reducing systematic errors.

10 Precision limit—space domain method

- Measure difference of beam polarization orientation at end of run minus at beginning of run.
- p-Carbon left/right scattering asymmetry polarimetry.
- This polarimetry is well-tested, “guaranteed” to work,
- but also “destructive” (measurement consumes beam)

particle	$\lvert d_{\mathrm{elec}} \rvert$ current upper limit e-cm	error after 10^4 pairs of runs e-cm
neutron	3×10^{-26}	
proton	8×10^{-25}	$\pm 10^{-29}$
electron	10^{-28}	$\pm 10^{-29}$

11 Resonant polarimetry—more detail next week

- Planned Stern-Gerlach electron polarimetry test(s)
- R. Talman, LEPP, Cornell University;
  B. Roberts, University of New Mexico;
  J. Grames, A. Hofler, R. Kazimi, M. Poelker, R. Suleiman;
  Thomas Jefferson National Laboratory
  2017 International Workshop on Polarized Sources,
  Targets & Polarimetry,
  Oct 16-20, 2017,

12 Precision limit—frequency domain method

- Frequency domain—"Fourier", "interferometry", "fringe counting", "resonamt" etc.
- Measure the spin tune shift when EDM precession is reversed
- Relies on phase-locked Stern-Gerlach polarimetry
- Like the Ramsey neutron EDM method.
- This polarimetry has not yet been proven to work.
- **This method cannot be counted on until resonant polarimetry has been shown to be practical.**

particle	$\lvert d_{\mathrm{elec}} \rvert$ current upper limit e-cm	excess fractional cycles per pair of 1000 s runs	error after 10^4 pairs of runs e-cm	roll reversal error e-cm
neutron	3×10^{-26}			
proton	8×10^{-25}	$\pm 8 \times 10^3$	$\pm 10^{-30}$	$\pm 10^{-30}$
electron	10^{-28}	± 1	$\pm 10^{-30}$	$\pm 10^{-30}$

13 Achievable precision (assuming perfect phase-lock)

- To make estimates more concrete, measure EDM in units of (nominal value) 10^{-29} e-cm $\equiv \tilde{d}$
- *The challenge is to measure an EDM value less than 1* (in units of 10^{-29} e-cm).
- 2 x EDM(nominal)/MDM precession rate ratio:
  $$2\eta^{(e)} = 0.92 \times 10^{-15} \approx 10^{-15}$$
- about the same as Pound-Rebka "falling" photon gravitational Mossbauer shift experiment
- "Frozen spin method" recovers "off the top" about 6 out of these 15 orders of magnitude

14 Achievable precision (continued)

- duration of each one of a pair of runs $= T_{\rm run}$
- smallest detectable fraction of a cycle $= \eta_{\rm fringe} = 0.001$
- small, but achieved in Pound-Rebka experiment

Using this terminology, the smallest meaningful non-zero detection is one fractional fringe. Then the EDM signal detected in a single run can be expressed as a number of fractional fringes N_{FF}. The result is

$$N_{FF} = \frac{\eta^{(p)}\tilde{d}}{\eta_{\rm fringe}}\, h_r f_0\, T_{\rm run} \quad \Big(\overset{\rm e.g.}{\approx} \ \frac{10^{-15}}{0.001}\, 100 \cdot (0.4 \times 10^6) \cdot 10^5\, \tilde{d} \approx 0.4\, \tilde{d} \Big). \tag{1}$$

- By this estimate, for $\tilde{d} = 1$, i.e. an EDM of 10^{-29} e-cm, a meaningful measurement can be obtained in a few days.
- But this assumes the existence of resonant polarimetry.
- Though under development, as discussed later, *resonant polarimetry has never been shown to be practical.*

15 Design requirements for proton EDM storage ring

- Measuring the proton electric dipole moment (EDM) requires an electrostatic storage ring in which 233 MeV, frozen spin polarized protons can be stored for an hour or longer without depolarization.
- The design orbit consists of multiple electrostatic circular arcs
  - Electric breakdown limits bending radius, e.g. $r_0 > 40\,\mathrm{m}$
  - For longest spin coherence time (SCT) and for best systematic error reduction the *focusing needs to be as weak as possible*
  - This is a "worst case" condition for electric and magnetic storage rings to differ (because kinetic energy depends on electric potential energy)
  - To reduce emittance dilution by intrabeam scattering (IBS) the ring needs to operate "below transition"
- Ring must be accurately clockwise/counter-clockwise symmetric
  - Accurately symmetric injection lines are required.
  - Initially single beams would be stored, with run-to-run alternation of circulation directions.
  - Ultimate reduction of systematic error will require simultaneously counter-circulating beams.

"Magic" central design parameters for frozen spin proton operation:

$$
\begin{aligned}
c &= 2.99792458e8\,\mathrm{m/s}\\
m_p c^2 &= 0.93827231\,\mathrm{GeV}\\
G &= 1.7928474 \;\; \text{anomalous magnetic moment}\\
g = 2G+2 &= 5.5856948\\
\gamma_0 &= 1.248107349\\
\mathcal{E} = \gamma_0 m_p c^2 &= 1.171064565\,\mathrm{GeV}\\
K_0 = \mathcal{E} - m_p c^2 &= 0.232792255\,\mathrm{GeV}\\
p_0 c &= 0.7007405278\,\mathrm{GeV}\\
\beta_0 &= 0.5983790721
\end{aligned}
$$

For mnemonic purposes it is enough to remember β_0 =0.6, $\gamma_0 = 1.25$, and p_0c=0.7 MeV.

17 Weak-weaker WW-AG-CF focusing ring design

- An ultraweak focusing, "weak/weaker, alternating-gradient, combined-function" (WW-AG-CF) electric storage ring is described.
- All-electric bending fields exist in the tall slender gaps between inner and outer, vertically-plane, horizontally-curved electrodes.

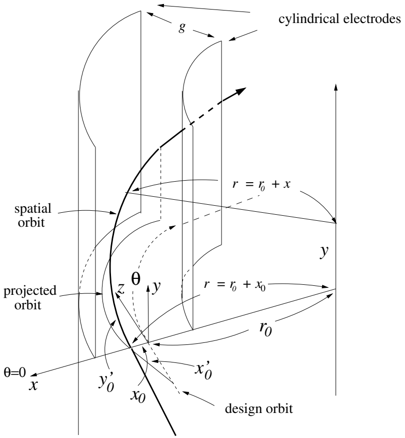

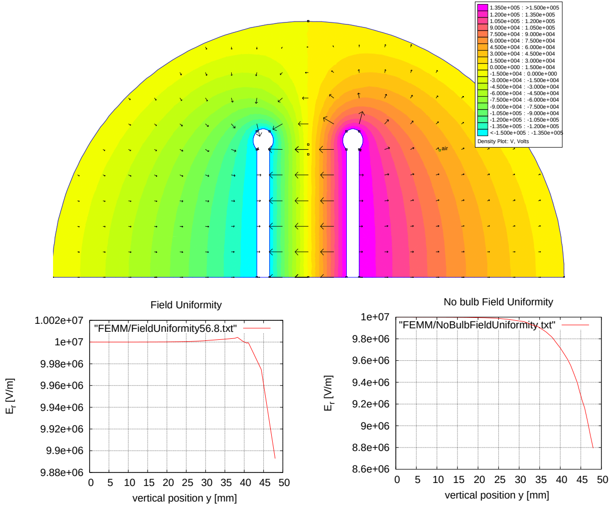

Figure 2: Above: Electrode edge shaping to maximize uniform field volume; Below left: bulb-corrected field uniformity; Below right: uncorrected field intensity. Only the top 5 cm is shown. The electrode height can be incresed arbitrarily without altering the electric field.

- The radial electric field dependence is

$$E = E_r \sim \frac{1}{r^{1+m}},$$

  where, ideally for spin decoherence, the field index m would be exactly $m = 0$.
- $m = 0$ (pure-cylindrical) field produces horizontal bending as well as horizontal "geometric" focusing, but no vertical force
- (Not quite parallel) electrodes, with m alternating between $m = -0.2$ and $m = +0.2$ provides net vertical focusing.
- Not "strong focusing", this is "weak-weaker" WW-AG-CF focusing, just barely strong enough to keep particles captured vertically.
- Beam distributions are highly asymmetric, much higher than wide, matching the good field storage ring aperture.

- (Not counting trims, nor slanted poles) there are no quadrupoles
- This is favorable for systematic electric dipole moment (EDM) error reduction. *There is no spin decoherence (for frozen spins) in a pure* $m = 0$ *field* — explained later
- The average particle speeds in drift sections do not need to be magic—because there is no spin precession in drift sections.
- Still, the dependence of revolution period on momentum offset is very small, making the synchrotron oscillation frequency small, and not necessarily favorable as regards being above or below transition.
- IBS stability requires below-transition operation, which requires quite long total drift length.

21 Total drift length condition for below-transition operation

- As with race horses, faster particles can lose ground in the curves but still catch up in the straightaways.
- To run "below transition", the sum of all drift lengths has to exceed $L_D^{\mathrm{trans.}}$, given in terms of dispersion D^O by

$$L_D^{\mathrm{trans.}} = 2\pi D^O \, \beta_0\gamma_0 \approx 1.5\pi D^O \approx 115\,\mathrm{m}.$$

- **On 17 December, 2017, I suddenly realized that there is a serious disagreement between my formalism and Valeri Lebedev's (and all other Wollnik 6x6 linearized transfer matrix user's) formalism concerning longitudinal dynamics.**
- (Naturally) I assume I am correct, but perhaps not.
- The disagreement has a huge impact on the detailed lattice design. But it does not seriously effect strategic EDM planning.
- **The disagreement has to be resolved.**
- I propose deferring this until the weak-weaker/weak/strong focusing discussion on Day 3.

22 Longitudinal γ variation on off-momentum orbits

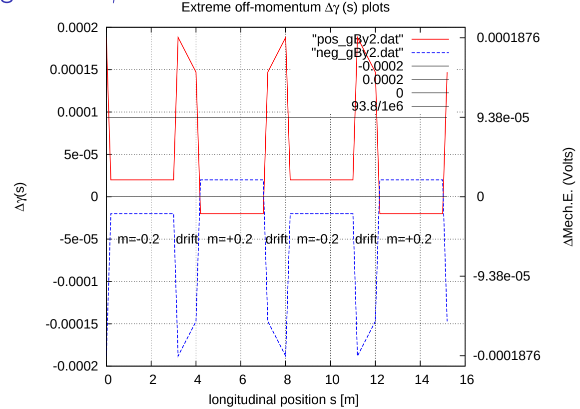

Figure 3: Dependence of deviation from "magic" $\Delta\gamma(s) = \gamma(s) - \gamma_0$ on longitudinal position s, for off-momentum closed orbits (circular arcs within bends) just touching inner or outer electrodes at $x = \pm 0.015\,\mathrm{m}$. *Notice the anomalous cross-overs in $m > 0$ bends.*

The dispersion is essentially positive everywhere, and the speed within bends is essentially the same for all particles. If the circumference fraction allotted to bends is close to 1, the revolution period will be dominated by momentum offset δ (rather than velocity offset). *This implies "above transition" operation.*

23 Off-momentum closed orbits

- For central radius r_0 the off-momentum radius is determined by Newton's centripetal force law

$$eE_0\left(\frac{r_0}{r}\right)^{1+m} = \frac{\beta pc}{r} \overset{\text{also}}{=} \frac{m_p c^2}{r}\Big(\gamma - \frac{1}{\gamma}\Big),$$

  where $r = r_0 + x_D$ is the radius of an off-momentum arc of a circle with the same center.
- For $m \neq 0$, r cancels, and the radius is indeterminant.
- A powerful coordinate transformation is:

$$\xi = \frac{x}{r} = \frac{x}{r_0 + x}$$

- For our typical values ($x = 1\,\mathrm{cm}$, $r_0 = 40\,\mathrm{m}$), for all practical purposes, ξ *can simply be thought of as* x *in units of* r_0..

- The electric field is then

$$\mathbf{E}(\xi) = -E_0\,(1-\xi)^{1+m}\,\hat{\mathbf{r}},$$

- Off-momentum closed orbits are “parallel” arcs of radius $r = r_0 + x_D$ inside a bend, entering and exiting at right angles to straight line orbits displaced also by x_D.
- The relativistic gamma factor on the orbit (inside) is γ^I, which satisfies

$$eE_0 r_0\,(1-\xi)^m = \beta^I p^I c = m_p c^2\Big(\gamma^I - \frac{1}{\gamma^I}\Big),$$

- This is a quadratic equation for γ^I *inside* bend.
- For $r \neq r_0$, because of the change in electric potential at the ends of a bend element, the gamma factor *outside* has a different value, γ^O.

- For $m \neq 0$ the orbit determination is no longer degenerate.
- Solving the quadratic equation for γ^I, the gamma factor is given by the positive root;

$$\gamma^I(\xi) = \frac{E_0 r_0 (1-\xi)^m}{2m_p c^2/e} + \sqrt{\left(\frac{E_0 r_0 (1-\xi)^m}{2m_p c^2/e}\right)^2 + 1}.$$

- This function is plotted next for $m = \pm 0.2$.

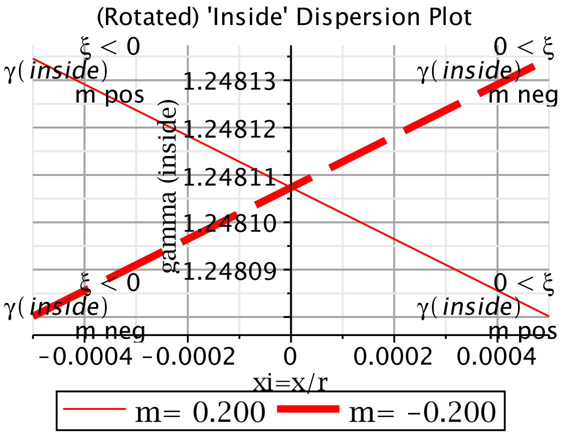

Figure 4: This figure shows a "dispersion plot" of "inside" gamma value γ^I plotted vs ξ. The curves intersect at the magic value $\gamma^I = 1.248107$. Because $d\gamma/d\beta = \beta\gamma^3$ is equal to about 1.17 at the magic proton momentum, the fractional spreads in velocity, momentum, and gamma are all comparable in value—in this case about $\pm 2 \times 10^{-5}$. This figure may be confusing, since it is rotated by 90 degrees relative to conventional dispersion plots. For this reason one should also study the following plot, which is identical except for being rotated, and is annotated as an aid to comprehension. Subsequent plots have the present orientation, however.

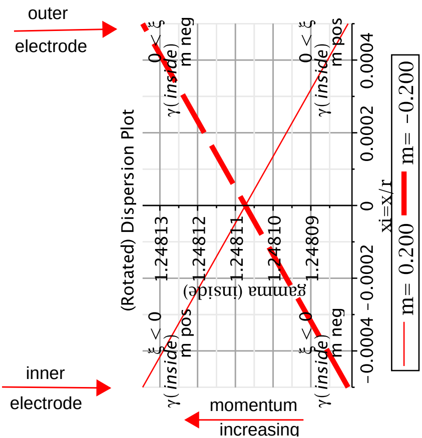

Figure 5: This plot is identical to the previous one except for being rotated by 90 degrees into conventional orientation (except momentum increases from right to left). It shows the dependence of $\xi = x/r$ vs "inside" gamma value γ^I, for $m = -0.2$ and $m = 0.2$. Note that, for $m < 0$ larger momentum causes larger radius while, for $m > 0$ the opposite is true. *What is striking is that the slope is opposite for $m > 0$ and $m < 0$. This is "anomalous".*

- Electric potential is defined to vanish on the design orbit
- Expressed as power series in ξ, the electric potential is

$$
\begin{aligned}
V(r) &= -\frac{E_0 r_0}{m}\Big((1-\xi)^m - 1\Big) \\
&= E_0 r_0\Big(\xi + \frac{1-m}{2}\xi^2 + \frac{(1-m)(2-m)}{6}\xi^3 \dots\Big). \qquad (2)
\end{aligned}
$$

- This simplifies spectacularly for the Kepler m=1 case. But we are concerned with the small $|m| << 1$ case.
- As a proton orbit passes at right angles from outside to inside a bend element, its total energy is conserved;

$$
\begin{aligned}
\gamma^O(\xi) &= \frac{\mathcal{E}^O}{m_p c^2} = \frac{\mathcal{E}^I}{m_p c^2} \\
&= \gamma^I(\xi) + \frac{E_0 r_0}{m_p c^2/e}\Big(\xi + \frac{1-m}{2}\xi^2 + \frac{(1-m)(2-m)}{6}\xi^3 \dots\Big).
\end{aligned}
$$

- Plots of $\gamma^O(\xi)$ for $m = \pm 0.2$ are shown next

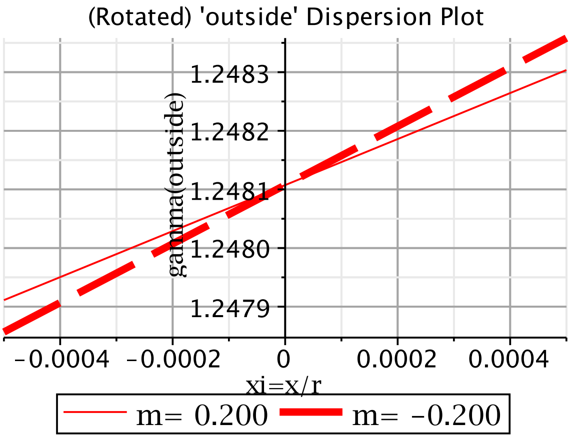

Figure 6: "Outside" dispersion plots. *Note that dispersion slopes are the same for $m < 0$ and $m > 0$.* Dependence of "outside" gamma value γ^O on $\xi = x/r$ for $m = -0.2$ and $m = 0.2$. Because $d\gamma/d\beta = \beta\gamma^3$ is equal to about 1.17 at the magic proton momentum, the fractional spreads in velocity, momentum, and gamma are all comparable in value—in this case about 2×10^{-4}. *The fractional spreads are an ordr of magnitude greater outside than inside.* This is *helpful*.

30 Parameter table

Table 1: Parameters for WW-AG-CF proton EDM lattice

parameter	symbol	unit	value
arcs			2
cells/arc	N_{cell}		20
bend radius	r_0	m	40.0
electric field	E_0	MV/m	10.483
electrode gap	gap	m	0.03
gap voltage	$\pm V_0$	KV	± 157.24
drift length	L_D	m	4.0
total drift length	L_{tot}	m	160
circumference	$\mathcal{C}$	m	411.327
field index	m		± 0.2
horizontal beta	β_x	m	40
vertical beta	β_y	m	2000
(outside) dispersion	D_x^O	m	24.4
horizontal tune	Q_x		1.64
vertical tune	Q_y		0.032
protons per bunch	N_p		2.5×10^8
horz. emittance	ϵ_x	μm	0.15
vert. emittance	ϵ_y	μm	0.25
(outside) mom. spread	$\Delta p^O/p_0$		$\pm 2 \times 10^{-4}$
(inside) mom. spread	$\Delta p^I/p_0$		$\pm 2 \times 10^{-5}$

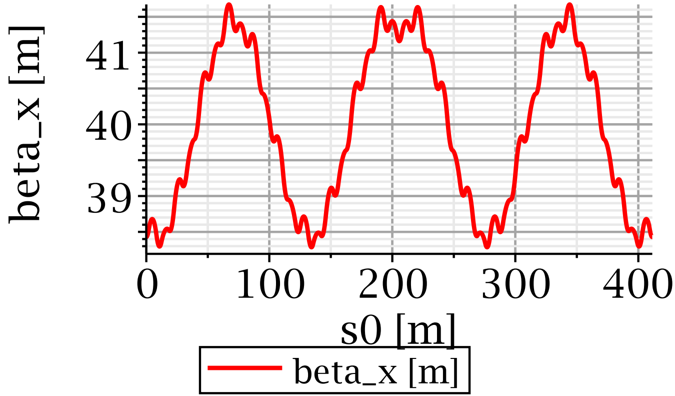

Figure 7: Horizontal beta function $\beta_x(s)$, plotted for full ring. For this case the total circumference is 411.3 m and the total drift length is L_D=160.0 m. Since this total drift length exceeds $L_D^{\mathrm{trans.}}$, the ring will be "below transition", as regards synchrotron oscillations.

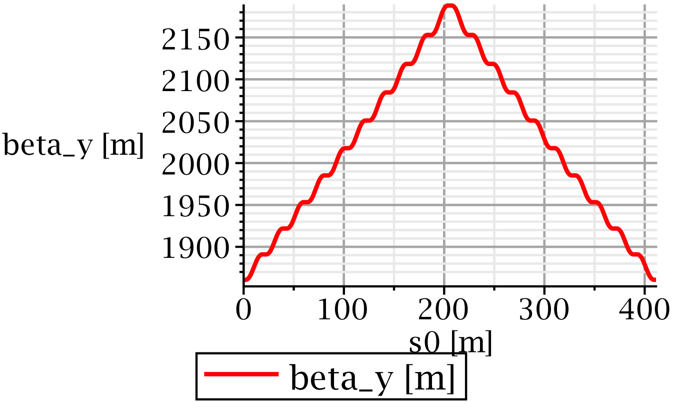

Figure 8: Vertical beta function $\beta_y(s)$, plotted for full ring. For this case the total circumference is 411.3 m and the total drift length is L_D=160.0 m. Since this total drift length exceeds $L_D^{\mathrm{trans.}}$, the ring will be "below transition", as regards synchrotron oscillations.

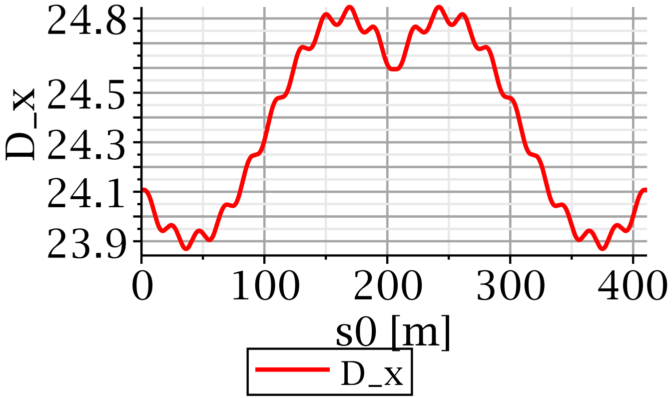

Figure 9: Outside dispersion function $D^O(s)$, plotted for full ring. For this case the total circumference is 411.3 m and the total drift length is 160.0 m.

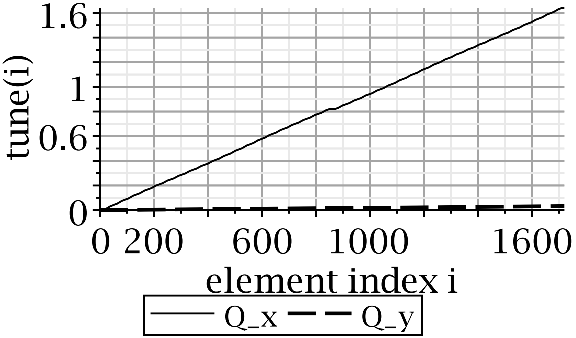

Figure 10: Transverse tune advances. The full lattice tunes are $Q_x = 1.640$ and $Q_y = 0.032$. Even smaller horizontal tune (for improved self-magnetometry) can be provided by trim quadrupoles, rather than by electrode shape or voltage adjustment, even consistent with zero net quadrupole focusing, but with octupole focusing for net vertical stability.

35 Self-magnetometry

- The leading source of systematic error in the EDM measurement is unintentional, unknown, radial magnetic fields.
- Acting on MDM, they cause spurious precession mimicking EDM-induced precession.
- (Apart from eliminating radial magnetic field) the only protection is to measure the differential beam displcement of counter-circulating beams.
- Greatest sensitivity requires weakest verticql focusing.
- i.e. extremely large value for β_y.
- or even octupole-only vertical focusing.

Current situation in Juelich

- Many significant advances:
  - highly polarized beam
  - electron cooling
  - stochastic cooling
  - spin tune determination accurate to 10 digits
  - phase locked beam polarization
  - long spin coherence time (in strong-focusing ring far from optimal for SCT)
  - machine position and powering stability over long times far superior to their absolute uncertainty
- still needed is a 450 m circumference electric ring (etc.)
- or low energy prototype proton EDM storage ring

- R. Talman, *The Electric Dipole Moment Challege,* IOP Publishing, 2017
- D. Eversmann et al., *New method for a continuous determination of the spin tune in storage rings and implications for precision experiments,* Phys. Rev. Lett. **115** 094801, 2015
- N. Hempelmann et al., *Phase-locking the spin precession in a storage ring,* P.R.L. **119**, 119401, 2017
- R. Talman, J. Grames, R. Kazimi, M. Poelker, R. Suleiman, and B. Roberts, *The CEBAF Injection Line as Stern-Gerlach Polarimeter,* Spin-2016 Conference Proceedings, 2016
- R. Talman, LEPP, Cornell University; B. Roberts, University of New Mexico; J. Grames, A. Hofler, R. Kazimi, M. Poelker, R. Suleiman; Thomas Jefferson National Laboratory; *Resonant (Logitudinal and Transverse) Electron Polarimetry,* 2017 International Workshop on Polarized Sources, Targets and Polarimetry, KAIST, Republic of Korea, 2017

- R. Li and P. Musumeci, *Single-Shot MeV Transmission Electron Microscopy with Picosecond Temporal Resolution,* Physical Review Applied 2, 024003, 2014
- Storage Ring EDM Collaboration, *A Proposal to Measure the Proton Electric Dipole Moment with* 10^{-29} *e-cm Sensitivity,* October, 2011
- G. Guidoboni et al., *How to reach a thousand second in-planepolarization lifetime with 0.97 GeV/c deuterons in a storage ring,* P.R.L. **117**, 054801, 2016
- M. Plotkin, *The Brookhaven Electron Analogue, 1953-1957,* BNL–45058, December, 1991
- S.P. Møller, *ELISA—An Electrostatic Storage Ring for Atomic Physics,* Nuclear Instruments and Methods in Physics Research A 394, p281-286, 1997
- S. Møller and U. Pedersen, *Operational experience with the electrostatic ring, ELISA,* PAC, New York, 1999

- S. Møller et al., *Intensity limitations of the electrostatic storage ring, ELISA*, EPAC, Vienna, Austria, 2000
- Y. Senichev and S. Møller, *Beam Dynamics in electrostatic rings*, EPAC, Vienna, Austria, 2000
- A. Papash et al., *Long term beam dynamics in Ultra-low energy storage rings*, LEAP, Vancouver, Canada, 2011
- R. von Hahn, et al. *The Cryogenic Storage Ring*, arXiv:1606.01525v1 [physics.atom-ph], 2016
- j. Ullrich, et al., *Next Generation Low-Energy Storage Rings, for Antiprotons, Molecules, and Atomic Ions in Extreme Charge States*,
- Loss of protons by single scattering from residual gas is discussed in detail in a paper Frank Rathmann drew to my attention: C. Weidemann et al., *Toward polarized anti-protons: Machine development for spin-filtering experiments*, PRST-AB **18**, 0201, 2015